Chapter 4

Modeling the Condensation of a Vapor Under Equilibrium and Non-Equilibrium Conditions

In this chapter, we describe the equations which govern the conservation of mass, momentum, energy and the phase change process of a real gas inside geometries like nozzles and ejectors. We discuss two different formulations available in the commercial flow solver Ansys CFX, namely, the equilibrium phase change solver and the classical nucleation theory based non-equilibrium phase change solver. These equations form the basis for the computational fluid dynamics based work on R-744 condensation performed in this thesis. The following discussion is based on the 121].

4.1 Introduction

High speed compressible flows with phase change are involved in a number of important industrial applications, like for example, the flow of steam through nozzles and turbine sections (Moses 102 101 105 106]); the flow of refrigerants 78 92], Giacomelli et al. 93 122]); the flow of Carbon dioxide inside compressors used in supercritical 123 97 98]); during the sudden fracture induced depressurisation of CO_2 pipelines used in carbon capture and storage (Brown 124 125 126]) etc. A common feature of

such flows is the phase change process under thermodynamic non-equilibrium conditions that prevail during the high speed expansion of the working fluid. The phase change process may be essential for the operation of the device, like for an ejector, while having undesirable effects on the performance of steam turbines and supercritical CO_2 compressors where it leads to blade erosion and vibration induced failure. The presence of shock waves, shear layers, boundary layer separation, turbulence along with the phase change process makes the flow inside such devices very complicated to be analysed with analytical and experimental methods. Another major difficulty is the presence of thermodynamic non-equilibrium condition which occurs universally in such flows. Under such a condition, the working fluid attains metastable thermodynamic states and suddenly undergo phase change process leading to what is known as a condensation shock. One also has to consider real gas effects while investigating the flow characteristics inside these devices. All these features make the experiments on compressible two phase flows with phase change a difficult task. Simulation of the compressible phase change process based on the computational fluid dynamics based techniques is a viable alternative to the experiments. It provides a detailed information on the flow field and the phase change process. In the following sections, we present the equations which govern the mass, momentum and energy conservation for a compressible fluid. We also discuss the equations which govern the phase change process of a vapor under homogeneous equilibrium and non-equilibrium conditions.

4.2 Governing Equations for Equilibrium Phase Change Solver

The equilibrium phase change model assumes that the inter-phase transport processes occur at a much faster time scale compared to the fluid flow time scale so that there exists a mechanical, thermal and chemical potential equilibrium between the phases. The consequences of this assumption are the equality of the velocity, pressure, temperature and the Gibbs free enthalpy of the phases in the grid cells containing both the phases. The two phases are treated as a single fluid mixture with different thermophysical properties depending on the spatial distribution of the individual phases. Because of the mechanical and the thermal equilibrium between the phases, the homogeneous equilibrium model does not require an explicit formulation of the interfacial transport processes. This approach is valid for simulating condensing vapor flows with small liquid fractions where the mixture of the two phases is not far from the thermodynamic equilibrium. In the following, the subscript l stands for the liquid phase, v stand for the vapor phase and m stands for their mixture.

The mass conservation equation for the two phase mixture is given by

$$\frac{\partial \rho_m}{\partial t} + \nabla \cdot \rho_m \vec{U} = 0, \tag{4.1}$$

where $\rho_m = \alpha_l \rho_l + \alpha_g \rho_g$ is the mixture density and α is the volume fraction of the phases with the constraint $\alpha_l + \alpha_g = 1$. The momentum conservation equation for the two phase mixture is given by

$$\frac{\partial \rho_m \vec{U}}{\partial t} + \nabla \cdot \rho_m \vec{U}\vec{U} = -\nabla p + \nabla \cdot \left\{ \mu_m (\nabla \vec{U} + \nabla \vec{U}^T) - \frac{2}{3}\mu_m \nabla \cdot \vec{U}\mathbf{I} \right\} + S_m, \tag{4.2}$$

where $\mu_m = \alpha_l \mu_l + \alpha_v \mu_v$ is the viscosity of the mixture and S_m holds any other relevant momentum source term if applicable. Instead of solving a single equation for the mixture enthalpy, Ansys CFX solves for two different 'total enthalpy' based equations for the liquid and the vapor phase. These equations are respectively given by

$$\frac{\partial \alpha_l \rho_l h_{t,l}}{\partial t} - \alpha_l \frac{\partial p}{\partial t} + \nabla \cdot \alpha_l \rho_l \vec{U} h_{t,l} = \nabla \cdot \alpha_l k_l \nabla T + \alpha_l \nabla \cdot \tau_l \cdot \vec{U} + Q_l, \tag{4.3}$$

$$\frac{\partial \alpha_g \rho_g h_{t,g}}{\partial t} - \alpha_g \frac{\partial p}{\partial t} + \nabla \cdot \alpha_g \rho_g \vec{U} h_{t,g} = \nabla \cdot \alpha_g k_g \nabla T + \alpha_g \nabla \cdot \tau_g \cdot \vec{U} + Q_g. \tag{4.4}$$

In the above equations, Q_l and Q_g denote the heat transfer to the respective phases across the interface which are not modelled with the help of any correlations. These terms are chosen to be large compared to the other terms in the equations. This causes the two phases to have the same temperature and imply a fast phase change process. The mass fraction of the vapor is calculated based on the enthalpy of the mixture using the following equation:

$$x = \frac{h_{\text{mix}} - h_{\text{sat,l}}(p)}{h_{\text{sat,v}}(p) - h_{\text{sat,l}}(p)}. \tag{4.5}$$

This implies that a grid cell contains sub-cooled liquid if $x < 0$, superheated vapor if $x > 1$ and the two phase mixture if $0 \leq x \leq 1$. The different thermophysical properties of the fluid are calculated based on the vapor mass fraction value.

4.3 Equations for the Non-equilibrium Phase Change Solver

The Classical Nucleation Theory based non-equilibrium phase change solver computes for the homogeneous nucleation and growth of droplets in a rapidly expanding, supercooled fluid vapor. This model differs from the equilibrium phase change model in that it calculates the droplet diameter and its number density as part of the solution. The mathematical formulation of the model involves equations for the continuous and the dispersed phase which are assumed to move at the same speed. In the following, the subscript c stands for the continuous phase which is the vapor phase in our case while the subscript d stands for the dispersed phase which is the condensed liquid phase in the form of droplets. The mass conservation equation for the

continuous phase is given by

$$\frac{\partial \alpha_c \rho_c}{\partial t} + \nabla \cdot \alpha_c \rho_c \vec{U} = -S_d - \alpha_c \hat{m}_d \mathbf{J}_d, \tag{4.6}$$

while that of the dispersed phase is given by

$$\frac{\partial \alpha_d \rho_d}{\partial t} + \nabla \cdot \alpha_d \rho_d \vec{U} = S_d + \alpha_d \hat{m}_d \mathbf{J}_d. \tag{4.7}$$

where S_d represents the interfacial mass transfer term, $\mathbf{J}_d$ is the critical nucleation rate and $\hat{m}_d$ is the nucleated droplet mass based on the critical radius $\hat{R}_d$. The constraint $\alpha_c + \alpha_d = 1$ applies

127] provides the

following expression for the critical nucleation rate

$$\mathbf{J}_d = q_c \frac{\rho_v^2}{\rho_l} \left(\frac{2\sigma(T_v)}{\pi m_m^3} \right)^{1/2} * e^{-\hat{G}b}, \tag{4.8}$$

where q_c is an empirical constant, m_m is the mass of a single molecule of the fluid, $\hat{G}b$ is the Gibbs number at the critical drop radius and is given by

$$\hat{G}b = \frac{16}{3} \frac{\pi \sigma^3(T_v)}{k_b T_v^3 \left[\rho_l R \ln\{\phi_{\text{ss}}(T_v)\}\right]^2}, \tag{4.9}$$

and finally, $\phi_{\text{ss}} = \frac{P_v}{P_{\text{sat}}(T_v)}$ is the supersaturation ratio.

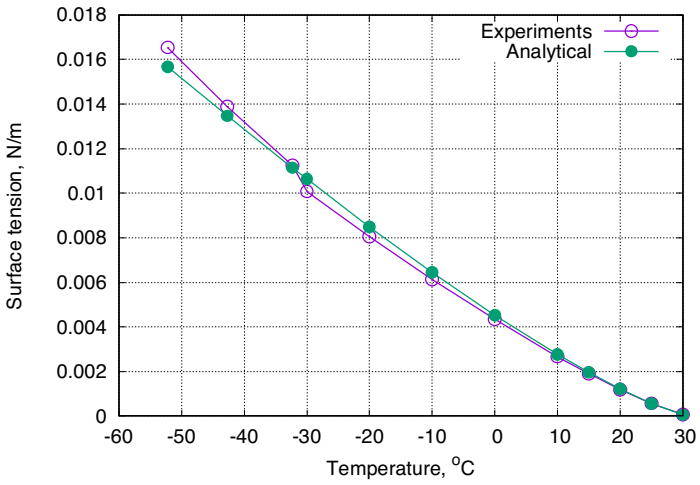

FIGURE 4.1: Variation of surface tension coefficient of R-744 with temperature. The analytical 128]. The experimental data is based on Jianxin and 129].

The surface tension coefficient σ between the liquid and the vapor states of R-744 is a function of temperature and is implemented in the current work based on the following equation from

128]

$$\sigma(T_r) = k_B T_{cr} \left(\frac{N_A}{V_{cr}}\right)^{2/3} * (4.35 + 4.14\omega) T_r^{1.26} * \left(1 + 0.19 T_r^{0.5} - 0.25 T_r\right), \tag{4.10}$$

where k_B is the Boltzmann constant, N_A is the Avogadro number, V_{cr} is the critical volume, ω is the accentric factor, $T_r = 1 - \frac{T}{T_{\text{cr}}}$ with $T_{\text{cr}} = 304.13$ K being the critical temperature of

4.10) and the actual

4.1 4.10 is implemented as a CEL expression

130 B.

The momentum conservation equation is similar to that for the homogeneous equilibrium model and is given by

$$\frac{\partial \rho_m \vec{U}}{\partial t} + \nabla \cdot \rho_m \vec{U}\vec{U} = -\nabla p + \nabla \cdot \left\{ \mu_m (\nabla \vec{U} + \nabla \vec{U}^T) - \frac{2}{3}\mu_m \nabla \cdot \vec{U}\mathbf{I} \right\} + S_m, \tag{4.11}$$

The continuous phase energy equation is given by

$$\frac{\partial \alpha_c \rho_c h_{t,c}}{\partial t} - \alpha_c \frac{\partial p}{\partial t} + \nabla \cdot \alpha_c \rho_c \vec{U} h_{t,c} = \nabla \cdot (\alpha_c \Gamma_t \nabla T) + S_H, \tag{4.12}$$

while that for the dispersed phase is given by

$$\frac{\partial \alpha_d \rho_d h_{t,d}}{\partial t} - \alpha_d \frac{\partial p}{\partial t} + \nabla \cdot \alpha_d \rho_d \vec{U} h_{t,d} = \nabla \cdot (\alpha_d \Gamma_t \nabla T) - S_H. \tag{4.13}$$

The equation governing the number density of the droplets is given by

$$\frac{\partial \rho_d N_d}{\partial t} + \nabla \cdot \rho_d \vec{U} N_d = \alpha_c \rho_d \mathbf{J}_d, \tag{4.14}$$

where the droplets are assumed to move at the mixture velocity because of the no slip condition between the phases. The droplet radius growth rate is given by

$$\frac{dR_d}{dt} = \frac{k_c}{R_d \rho_d (1 + \xi\,\text{Kn})} \left(\frac{T_d - T_c}{h_c - h_d}\right), \tag{4.15}$$

where ξ is an empirical constant and Kn is the Knudsen number which is included to take into account the droplet size variation from the molecular to the continuum scales. For small droplets ($d \leq 1\mu$m), the droplet temperature T_d is calculated using

$$T_d = T_{\text{sat}}(p) - T_{\text{sup}} \frac{R_d^*}{R_d}, \tag{4.16}$$

where $T_{\text{sat}}(p)$ is the saturation temperature as a function of pressure p, T_{sup} is the supercooling level in vapor phase, R_d is the droplet radius, and finally, R_d^* is the critical droplet radius. Here it may be noted that the equations discussed above require fluid thermophysical properties in

the subcooled state. This necessitates the use of a property database or an equation of state for the vapor phase amenable to extrapolation in the subcooled region. As per the Ansys solver 121], the IAPWS database for water and the Redlich-Kwong family of equation of state for CO_2 are capable of such extrapolations but the latter's accuracy is not reliable near the critical point and for subcooled liquid states. For R-744, we also extract the various 99]. A FORTRAN based code is developed for this purpose.

4.6 4.7) related to mass transfer across the interface are calculated by

$$S_d = \rho_d \beta_d \frac{dR_d}{dt}, \tag{4.17}$$

where $\beta_d = \frac{3\alpha_d}{R_d}$ is the interfacial area available per unit volume. The source terms in the 4.12 4.13), are given by

$$S_H = -S_d H_u + \beta_d Q_d, \tag{4.18}$$

where H_u is the upwinded total enthalpy whose value depends on the direction of mass transfer across the interface. The very small droplets ($R_d \leq 1\mu$) are assumed to have a uniform temperature with all the heat transfer Q_d occurring in the continuous phase during evaporation and condensation. The heat flux is calculated based on

$$Q_d = \frac{k_c}{R_d(1 + \xi\, Kn)}(T_d - T_c). \tag{4.19}$$

These governing equations are solved in Ansys CFX using a control volume based finite element method (CVFEM). Although Ansys CFX is capable of handling general unstructured grids, we used block-structured, curvilinear body-fitted grids in the current work for better accuracy and convergence behavior. In the next chapter, we present the results on the validation of the solver settings by simulating the phase change of R-744 and water inside converging-diverging nozzles.

4.4 Summary

In this chapter, we figured out the equations which govern the phase change process of a vapor during compressible high speed flows. These are the mass, momentum and energy conservation equations for the two phase mixture expressed in the differential form. There are extra equations relevant to the non-equilibrium flow solver which is based on the classical nucleation theory. These equations are for the critical nucleation rate, critical radius, critical Gibbs free energy change and the heat transfer during the phase change process etc. Most important is the equation for the variation of surface tension coefficient between the two R-744 phases as a function of

temperature. The R-744 surface tension values based on an equation are finally compared with the experimental data from literature.